

# “Experimental Investigation Of Mixed Convection With Water-Al<sub>2</sub>O<sub>3</sub> & Hybrid Nanofluid In Inclined Tube For Laminar Flow”

Gaffar G. Momin

**ABSTRACT:** Two experiments were carried out. first to study mixed convection Al<sub>2</sub>O<sub>3</sub> water nano fluid inside an inclined copper tube surface. The effects of nanoparticles concentration and power supply on the development of the thermal field are studied and discussed under laminar flow condition. Results show that the experimental heat transfer coefficient decreases slightly with an increase of particle volume concentration from 0 to 4%. Two new correlations are proposed to calculate the Nusselt number in the fully developed region for horizontal and vertical tubes volume concentrations up to 4%. and In second experimental work, a fully developed laminar convective heat through a uniformly heated circular tube using Al<sub>2</sub>O<sub>3</sub>-Cu/water hybrid nanofluid is presented. For this we synthesized Al<sub>2</sub>O<sub>3</sub>-Cu nanocomposite powder in a thermo chemical route that involves a hydrogen reduction technique and then dispersed the prepared hybrid nano powder in deionised water to form a stable hybrid nanofluid of 0.1% volume concentration. The convective heat transfer experimental results showed a maximum enhancement of 13.56% in Nusselt number at a Reynolds number of 1730 when compared to Nusselt number of water. The experimental results also show that 0.1% Al<sub>2</sub>O<sub>3</sub>-Cu/ water hybrid nanofluids have slightly higher friction factor when compared to 0.1% Al<sub>2</sub>O<sub>3</sub>/water nanofluid. The empirical correlations proposed for Nusselt number and friction factor are in good agreement with the experimental data.

**Keywords:** Heat transfer, Laminar flow, Mixed convection, Nanofluid, Nanoparticles, Al<sub>2</sub>O<sub>3</sub>-water mixture, Al<sub>2</sub>O<sub>3</sub>-Cu hybrid nano particles, Hydrogen reduction technique, Laminar flow, Hybrid nanofluid, Heat transfer enhancement, Friction factor.

## 1. Introduction

Modern nanotechnology has permitted the fabrication of materials with average size below 50nm. Fluids formed of saturated liquid and suspended nanoparticles are called nanofluids, a term first used by Choi [1]. Relevant experimental data has shown that nanofluids possess superior heat transfer properties compared to those of ordinary fluids. Such studies also indicate that these suspensions are relatively stable because of the very small particle size. Thus, nanofluids can constitute a promising alternative for advanced thermal applications, in particular for micro/nano-heat transfer applications where the current tendency towards smaller and lighter heat exchanger systems is considerable. It is worth mentioning that Khaled & Vafai have studied the effect due to thermal dispersion on the heat transfer characteristics of nanofluids. Their numerical results have shown that the presence of dispersive elements resulted in a 21% augmentation of the Nusselt number for a uniform heated tube.

However, there are no general models which may satisfactorily explain the strong heat transfer enhancement due to nanofluids as well as to accurately determine their properties. Most of the first experimental and theoretical studies were conducted to determine the nanofluid effective thermal conductivity. Some studies also provide data for the nanofluid effective viscosity. For forced convective heat transfer, Pak & Cho [11] studied the heat transfer behaviour in heated tubes and observed that, for a given Reynolds number, the convective heat transfer coefficient increases with increasing particle volume concentration. They provided the first correlation for computing the Nusselt number for turbulent regime. Li & Xuan [16] investigated experimentally the convective heat transfer and flow characteristics in a tube with a constant heat flux at the wall. From data collected on nanofluids composed of water and Cu, TiO<sub>2</sub> and Al<sub>2</sub>O<sub>3</sub> particles, they proposed empirical correlations for the Nusselt number in both laminar and turbulent flows. Wen & Ding [17] investigated the heat transfer performance of water-Al<sub>2</sub>O<sub>3</sub> mixture under laminar flow regime in a copper tube with 4.5 mm inner diameter. They found that the convective heat transfer coefficient increases with increasing Reynolds number and particles concentration. Furthermore, the improvement of the heat transfer coefficient was large in the entrance region of the horizontal heated tube. The nanofluids give a higher heat transfer coefficient than the base fluid for given Reynolds number, and such enhancement becomes more significant with an augmentation of particle concentration. For buoyancy-driven flows and heat transfer using nanofluids, very few studies have been carried out. Ben Mansour et al. [20] studied numerically the conjugate problem of laminar mixed convection flow of Al<sub>2</sub>O<sub>3</sub> water nanofluid in a uniformly heated inclined tube. They found that the presence of nanoparticles intensifies the buoyancy-induced secondary flow, especially in the developing region.

- Gaffar G. Momin. ( M.E.Heat Power )
- Assistant Professor in Mechanical Engineering , Pimpri Chinchwad College Of Engineering,Pune, INDIA-411044
- Email- [gaffarmomin01@gmail.com](mailto:gaffarmomin01@gmail.com)

## 2. First Experimental apparatus

Fig. 1 shows a schematic illustration of the experimental system used.

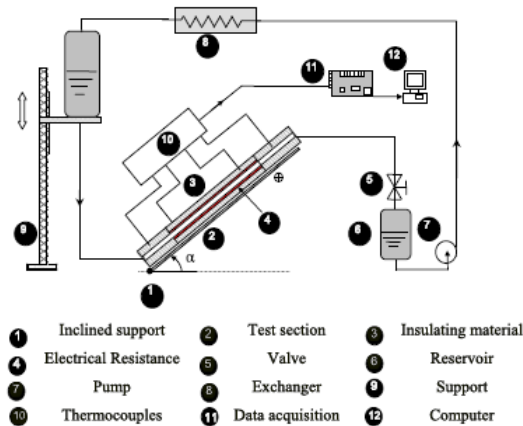


Fig. 1. Schematic representation of the experimental system.

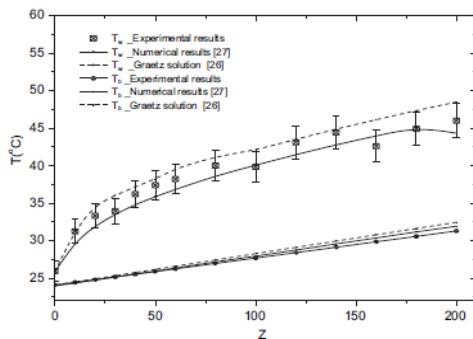


Fig. 2. Axial development of wall and fluid bulk temperatures for forced convection.

The fluid, distilled water or a nanofluid, flows down from an upper constant level tank and enters the heated section. The latter is a copper tube of internal diameter  $D \approx 6.35$  mm and total length of 2.24 m. The tube is submitted to a constant and uniform wall heat flux applied over a large portion of it,  $L_2 \approx 200D$ . The heating was realized using a standard flat-ribbon-type electrical resistance (Omega, USA) of 2 m in length and 12 mm in width. This resistance is rolled on the tube outer surface at constant pitch. A precise potentiometer was used to adjust, if necessary, the output voltage supplied to the resistance. In order to be able to create appropriate boundary conditions for both the tube inlet and outlet, two adiabatic sections with respective lengths of  $L_1 \approx 50D$  and  $L_3 \approx 100D$  are installed, one preceding the heated section and the other one immediately after it. Hence, after traversing the first long adiabatic section served as a hydrodynamic developing section, the fluid would have a parabolic axial velocity profile at the entrance of the heated section. In order to reduce heat losses towards the surrounding environment, a thick layer (2 cm) of fiber-glass insulating blanket was wrapped around the tube-and-resistance system. After traversing the test tube, the fluid passes through a valve and finally reaches the second lower collecting reservoir. Using a magnetic-driven centrifugal pump (MD-20RZ model from IWAKI), the fluid collected in the lower reservoir is then pumped upwards and traverses a tubular spiral-type

heat exchanger where heat is released towards a constant temperature cold water source. A desired flow rate of the liquid has been achieved by appropriately adjusting the height at which is fixed the upper reservoir. The fluid mass flow rate, which is measured using a classical and reliable 'stop-watch-and-weighting' technique, can be determined with accuracy as good as  $\pm 3\%$ . The heating electrical power, indirectly deduced from the measured voltage and current supplied using a precise multi-meter, can be determined with an accuracy of  $\pm 3\%$ . For the measurement of temperature at various places in the system, many thermocouples with an accuracy of  $\pm 0.1$  °C were installed: - 18 surface-type thermocouples were glued on the outer surface of the tube using a high-temperature cement-type compound among them, 14 T-type thermocouples were placed along the heated section and 4 others of J-type were fixed in the two adiabatic sections. All these thermocouples serve to monitor wall temperatures along the tube. - 3 other J-type thermocouples were fixed at different locations on the outer surface of the insulating layer. The measured temperatures were used to calculate the heat losses towards ambient air. For all the cases performed in this study, these heat losses did not exceed 4% of the total heat input, which are quite acceptable in junction with experimental uncertainties. - 2 other T-type thermocouples were used to measure fluid temperatures at the tube inlet and outlet. These thermocouples, made of stainless steel, have a very small diameter to minimize the obstruction of the flow. All the thermocouples and sensors were connected to a data acquisition system composed of an SCXI-1102 module, an SCXI-1303 terminal and an acquisition board; all these components were from National Instrument. The SCXI-1303 terminal possesses an internal thermistor for an automatic cold junction correction. The standard LabView software, also from National Instrument, was employed to perform the data acquisition and treatment.

## 3. Validation tests of the experimental system

This first set of tests was carried out using distilled water for a laminar 'pure' forced convection flow as well as for mixed convection flow. Fig. 2 shows a comparison of the axial development of wall and fluid bulk temperatures obtained theoretically, numerically [26] and experimentally for flow of water in a horizontal tube with a power supply of  $P \approx 185.94$  W  $\pm 5\%$  and a mass flow rate of  $m_0 \approx 3.1$  g/s  $\pm 3\%$ . The corresponding values of the Reynolds and Grashof's numbers are  $Re = 620$  and  $Gr = 4.50 \times 10^4$ . Therefore, the Richardson number is quite low ( $Ri = 0.1$ ) and these conditions correspond to forced convection flow. The agreement between the results can be qualified as satisfactory. For a mixed convection case, the experimental results of the convective heat transfer convection coefficient were compared with the values obtained from the numerical study [20] and from the Petukhov & Polyakov equation [27]. As shown in Fig. 3, there is good agreement between the experimental values of the Nusselt number and the other results [20,25], suggesting that the experimental apparatus performs quite satisfactorily.

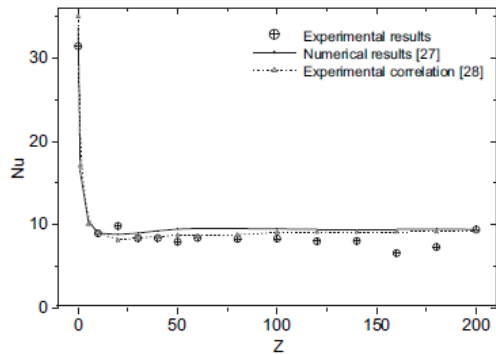


Fig. 3. Axial development of Nusselt number for mixed convection ( $Re = 360$ ,  $Gr = 7.3 \times 10^4$ ,  $Pr = 7$ ).

#### 4. Results and discussion of first experiment

The experiments were carried out using  $Al_2O_3$  water mixtures, with particles of average diameter 36 nm and for the following ranges of governing parameters: the power supply  $P$  between 190W and 420W, the particle volume fraction  $\phi$  from 0% to 4% and two tube inclinations. The results and discussion presented hereafter focus on the effects of particle volume concentration on the flow and heat transfer behaviour of the nanofluid both in the entrance and the fully developed regions. It is worth noting that in the thermally developed region, the difference between local and the corresponding bulk fluid temperatures is a function of the radial position only and the axial variation of fluid temperature is linear. 4.1. Effect of particle volume concentration on the development of the thermal field Fig. 4 shows the axial development of the wall temperature,  $T_w$ , and the fluid bulk temperature,  $T_b$ , for three particle volume concentrations, a power supply  $W$  and a mass flow. One can observe that both wall and bulk temperatures increase with increasing particle volume concentration. This is consistent with equation (1) which shows that the bulk temperature increase is inversely proportional to the heat capacity  $C_p$ . At a short distance from the end of the heated section, both  $T_w$  and  $T_b$  tend to the same value that depends on the overall heat balance.

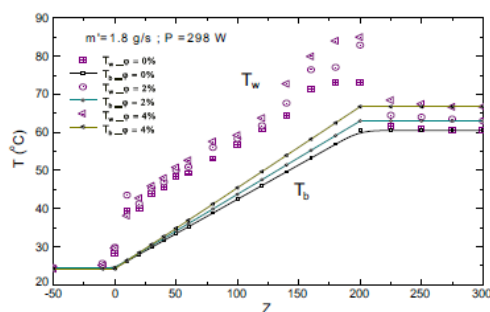


Fig. 4. Effect of particle concentration on axial development of temperatures ( $P = 298$  W,  $m' = 1.8$  g/s).

Results in Fig. 4 also show that the difference between fluid and wall temperature,  $T_w - T_b$ , increases slightly with an increase of  $\phi$ , which indicates that there is a slight decrease of the heat transfer coefficient (see Fig. 5).

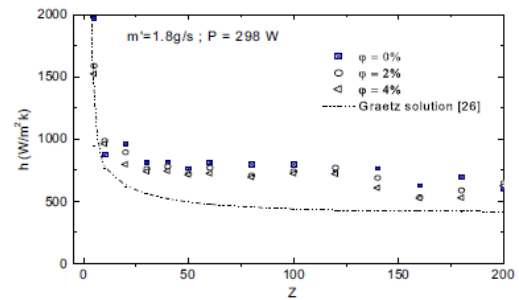


Fig. 5. Effect of particle concentration on axial development of heat transfer coefficient ( $P = 298$  W,  $m' = 1.8$  g/s).

Thus, for  $\phi$  increasing from 0 to 4%, an approximate decrease of 10% of the heat transfer coefficient has been obtained. However, as indicated in Fig. 5, its value remains higher than the corresponding value for forced convection. It appears therefore that, for the same mass flow rate and power supply, an increase of the particle volume concentration results in a degradation of the secondary motion caused by the buoyancy force. The reason for this is that the inclusion of suspended particles results in an important augmentation of the dynamic viscosity with respect to that of pure water, especially for high particle volume concentrations. These results show that the heat transfer behaviour of the nanofluid is not characterized only by the effective thermal conductivity. The other physical properties (density, thermal expansion coefficient, heat capacity) can affect the heat transfer characteristics of nanofluids in the forced convection [28] and free convection [29] as well. Thus, from equations (2) for an increase of the particle volume concentration from 0% to 4%, the effective thermal conductivity increases by 12%, the expansion coefficient decreases by 14% while the dynamic viscosity significantly augments by nearly 48%. 4.2. Effect of power supply on the development of the thermal field Figs. 6 and 7 show the axial development of the wall temperature  $T_w$ , the fluid bulk temperature  $T_b$  and of the heat transfer coefficient for various values of power, is very interesting to observe that due to axial heat conduction in the tube wall, the imposed heat flux clearly affects both adiabatic zones. In the upstream adiabatic zone, values of  $T_w$  are superior to  $T_{in}$ . The wall temperatures increase steeply up to the location  $Z = 50$  because of the development of the thermal field. Beyond this position, the fully developed conditions are reached and all temperatures increase linearly with the axial coordinate. At a short distance from the end of the heated section, both  $T_w$  and  $T_b$  tend to the same value that is dependent on the overall heat balance. Results in Fig. 6 also show that the temperature difference  $T_w - T_b$  increases with an increase of  $P$ . This behaviour is explained by the fact that for given values of  $\phi$  and  $m_0$ , an increase of power supply implies a higher wall heat flux  $q_0$  and therefore, results in a more pronounced secondary flow. Thus in the fully developed flow zone, the heat transfer coefficient has increased by nearly 18%. It is worth noting that the heat transfer coefficient reaches a minimum value approximately at the location  $Z = 50$ , which indicates that the buoyancy effect in the region becomes more intense. A similar behaviour has been observed numerically by Ben Mansour et al. [26] for mixed convection in a horizontal tube.

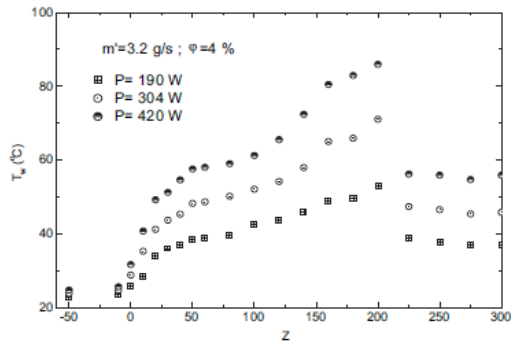


Fig. 6. Effect of heating power on axial development of wall temperature.

#### 4.3 Correlation for Nusselt number:

The heat transfer behaviour of the nanofluid is characterized by various factors such as thermal conductivity, heat capacity, thermal expansion coefficient, viscosity, particle volume concentration and tube inclination. Using the experimental data, the following correlation was determined for the Nusselt number in a horizontal tube as a function of the particle volume concentration ( $0 < \alpha < 4\%$ ). The correlation coefficient, the maximum and average error are 96.5%, 5% and 2% respectively. These values show that the proposed correlation is satisfactory within the specified ranges of the independent parameters. For the vertical tube, a new correlation expressing the Nusselt number as a function of the Grashof and Reynolds numbers is as follows: This correlation exhibits maximum and mean errors of 6% and 2.5% respectively while the correlation coefficient is 94%. The two proposed correlations are in very good agreement with experimental results for flow of nanofluids in a horizontal and vertical tube.

### 5. Second Experimental Study:

5.1. Preparation of nanofluid and thermophysical properties  
Preparation of nanofluids is the first key step in experimental studies. In the present work, Al<sub>2</sub>O<sub>3</sub>-Cu/water hybrid nanofluid of volume fraction 0.1% was prepared using two step method. Specified amount of Al<sub>2</sub>O<sub>3</sub>-Cu nanoparticles were dispersed in deionized water with sodium lauryl sulfate (SLS) as dispersant by using an ultrasonic vibrator (Lark, India) generating ultrasonic pulses in the power of 180W at 40 kHz. To get a uniform dispersion and stable suspension, which determine the final properties of nanofluids, the nanofluids were kept under ultrasonic vibration continuously

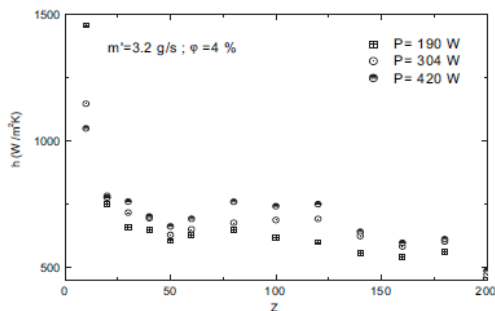


Fig. 7. Effect of heating power on axial development of heat transfer coefficient.

for 6 h [19]. Stability of the prepared nanofluid was studied by measuring the pH values. The pH was measured using a pH meter (Deep Vision: Model 111/101) and the values were found to be around 5.5 which is far from the isoelectric points (IEP) of alumina and copper nanoparticles. This ensured that the nanoparticles were well dispersed and the nanofluid was stable because of very large repulsive forces among the nanoparticles when pH is far from isoelectric point. The key parameters for assessing the heat transfer merits of nanofluids are their thermophysical properties. Among measuring various thermophysical properties, thermal conductivity is generally regarded as most difficult property to be measured due to large errors associated during the measurement. The thermal conductivity of Al<sub>2</sub>O<sub>3</sub>-Cu/water hybrid nanofluid was measured by using a KD2 Pro thermal properties analyser (Decagon Devices, Inc., USA). It consists of a handheld microcontroller and sensor needles. The KD2's sensor needle contains both a heating element and a thermistor. The controller module contains a battery, a 16-bit microcontroller/AD converter, and power control circuitry. The sensor needle used was KS-1 which is made of stainless steel having a length of 60 mm and a diameter of 1.3 mm and closely approximates the infinite line heat source which gives least disturbance to the sample during measurements. Each measurement cycle consists of 90 s. During the first 30 s, the instrument will equilibrate which is then followed by heating and cooling of sensor needle for 30 s each. The temperature rise observed during 30 s of heating time was in the range of 0.3–0.4 °C (0.01–0.0133 °C/s). This ensures that the heat pulse given by the sensor needle is very small and hence, thermally driven convection currents in the sample are eliminated which in turn avoids any disturbances in the sample during measurements. At the end of the reading, the controller computes the thermal conductivity using the change in temperature (DT) – time data from where q is constant heat rate applied to an infinitely long and small “line” source, DT1 and DT2 are the changes in the temperature at times t1 and t2 respectively. The KD2 Pro analyzer used in our experiments collects data at 1 s intervals during a 30 s heating time and a 30 s cooling time. The final 20 points during heating and cooling are used in a simultaneous least squares computation which determines the thermal conductivity. Temperature is measured by a 16 bit analog to digital converter. All the computations are done by an internal 16 bit microcontroller and the result is displayed. The measure of how well the measured data fits with the model given in Eq. (1) is represented by R2 value that is shown in the display screen of the microcontroller. As a good data set will give R2 values above 0.9990, the measured data were discarded if the R2 value is less than 0.9990 during the experiments. The calibration of the sensor needle was carried out first by measuring thermal conductivity of distilled water, glycerine and ethylene glycol. Nanofluid samples of 45 ml were taken in a vial of 30 mm diameter whose cap is equipped with a septum through which the sensor needle was inserted. For accurate measurements, the needle was inserted fully into the fluid, and oriented vertically and centrally inside the vial without touching the side walls of the vial. Insertion of the sensor needle probe into the fluid in this orientation will minimize errors from free convection. In addition, the vial of nanofluid was turned upside down on the top of the needle

so that any bubbles in the fluid would float to the top away from the needle. The thermal conductivity for each volume concentration of the nanofluid was measured at an interval of 15 min for a period of about 3 h after sonication. 15 min time was allowed between successive measurements for the temperature of the sensor needle and sample to re-equilibrate. The average of data points that did not appreciably vary over the last 1 h is taken as the thermal conductivity value in heat transfer calculations of this work. The viscosity of the nanofluid was measured using Brookfield cone and plate viscometer (LV/DV-I PRIME C/P) supplied by Brookfield engineering laboratories of USA. The thermophysical properties of 0.1% Al<sub>2</sub>O<sub>3</sub>-Cu/water hybrid nanofluid were estimated as follows:

thermal conductivity  $k = 0.62 \text{ W/m K}$ ,

viscosity = 0.93 cP,

density = 1001.3 kg/m<sup>3</sup> and

specific heat = 4176.83 J/kg -K.

## 5.2. Heat transfer experimental setup

The schematic diagram of the experimental setup is shown in Fig. 8. The experimental set up consists of a calming section, test section, pump, cooling unit, and a fluid reservoir. Calming section made of straight copper tube with the dimension 1000 mm long, 10 mm ID and 12 mm OD is used to eliminate the entrance effect. A straight copper tube of 1000 mm long, 10 mm ID and 12 mm OD is used as test section. The test section tube is wound with ceramic beads coated electrical SWG Nichrome heating wire of resistance 120  $\Omega$ . Over the electrical winding a thick insulation is provided using glass wool to minimize heat loss. The terminals of the Nichrome wire are attached to an auto-transformer using which heat flux can be varied by varying the voltage.

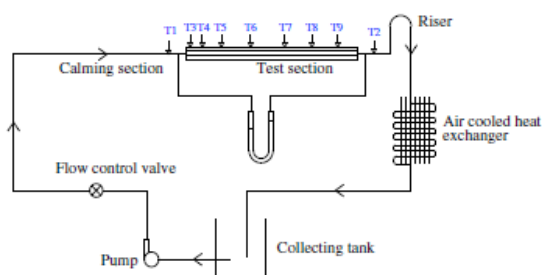


**Fig.8** Schematic diagram of Heat Transfer Experimental Set Up.

Calibrated RTD PT 100 type temperature sensors of 0.1  $^{\circ}\text{C}$  accuracy are placed in the thermo wells mounted on the test section at axial positions of 50, 100, 200, 300, 500, 700 and 950 mm from the inlet of the test section to measure the outside wall temperatures. The entry and exit temperatures of the fluid are measured by using two calibrated RTD PT 100 type temperature sensors immersed in the mixing chambers provided at the inlet and exit. A differential u-tube manometer is fitted across the test section to measure the pressure drop in the test section.

The fluid after passing through the heated test section flows through a riser section and then through the cooling unit which is an air cooled heat exchanger and finally it is collected in the reservoir. A peristaltic pump (RH-P120I, Ravel Hiteks Pvt. Ltd.) is used to circulate the fluid through the circuit. The pump discharge is varied by adjusting the speed of rotation. The pump gives a maximum discharge of 2.55 l per minute. A plastic container of 5 l capacity is used as the fluid reservoir.

## 6. Results and discussions of second experiment

### 6.1. Heat transfer study

The experimental data of Al<sub>2</sub>O<sub>3</sub>-Cu/water hybrid nanofluid of 0.1% volume concentration was used to deduce the Nusselt number and friction factor in laminar flow regime. Fig. 9 shows the comparison of Nusselt number of Al<sub>2</sub>O<sub>3</sub>-Cu/water hybrid nanofluid with the Nusselt number of water and 0.1% Al<sub>2</sub>O<sub>3</sub>/water nanofluid. The Nusselt numbers are calculated from the measured values of mean wall temperature and bulk mean temperature and the actual heat flux. The experimental results clearly show that the nanoparticles suspended in water increases the Nusselt number even for a very low volume concentration of 0.1%. The reasons for such increases in Nusselt number are reported in previous research works [8–10,24]. First of all, the convective heat transfer enhancement of water based Al<sub>2</sub>O<sub>3</sub>-Cu hybrid nanofluids may be attributed to the effective thermal conductivity enhancement of water based Al<sub>2</sub>O<sub>3</sub>-Cu hybrid nanofluids because the heat transfer coefficient,  $h$  is proportional to thermal conductivity,  $k$ . The experimental results also indicate that the presence of nanoparticles in the flow influences the heat transfer beyond what would be expected from increased thermal conductivity alone.

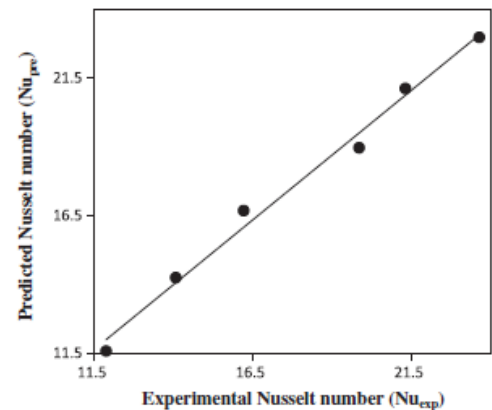


**Fig.9** comparison of Nusselt number of Al<sub>2</sub>O<sub>3</sub>-Cu/water hybrid nanofluid with the Nusselt number of water and 0.1% Al<sub>2</sub>O<sub>3</sub>/water nanofluid.

Thus, the thermal conductivity enhancement has a small effect on the enhancement of convective heat transfer coefficient. In addition, the thermal conductivity under dynamic condition may be much higher than that under static condition. Particle movement into centerline of a tube due to Brownian diffusion and thermophoresis significantly increases the viscosity and thermal conductivity of

nanofluids near the centerline. As a consequence of the viscosity increase of nanofluids near the centerline, velocity profile is flattened. The flattened velocity profile decreases the difference between the average tube wall temperature and bulk mean temperature of nanofluids under the constant heat flux. So the decrease in the difference between average tube wall temperature and bulk mean temperature of nanofluids together with a small thermal conductivity enhancement of nanofluids cause a very significant convective heat transfer coefficient of Al<sub>2</sub>O<sub>3</sub>-Cu/water hybrid nanofluids. The experimental results of hybrid nanofluid for laminar flow showed a maximum enhancement of 13.56% in Nusselt number at a Reynolds number of 1730 when compared to water. The average increase in Nusselt number for Al<sub>2</sub>O<sub>3</sub>-Cu/water hybrid nanofluid is 10.94% when compared to pure water. The enhancement obtained by 0.1% Al<sub>2</sub>O<sub>3</sub>/water nanofluid is 6.09% when compared to pure water. This means that the incorporation of a small amount of copper nanoparticles in alumina matrix significantly enhances the Nusselt number. The convective thermal resistance in forced convection heat transfer was evaluated in the case of different fluids. The thermal resistance to convective heat transfer of hybrid nanofluid was found to be less than that of alumina/water nanofluid and water. The difference between the measured average bulk temperature of the fluid and wall temperature at all Reynolds numbers were calculated for water, Al<sub>2</sub>O<sub>3</sub>/water nanofluid and Al<sub>2</sub>O<sub>3</sub>-Cu/water hybrid nanofluid. It was found that the difference between the measured average bulk temperature of the fluid and wall temperature is minimum in the case of Al<sub>2</sub>O<sub>3</sub>-Cu/water hybrid nanofluid.

## 7. Conclusion:

### 7.1 For first experiment

In this study, we have investigated experimentally the problem of thermally developing laminar mixed convection flow of water and water/Al<sub>2</sub>O<sub>3</sub> mixture inside an inclined tube with a uniform wall heat flux on its outside surface. The results have clearly shown that the presence of nanoparticles produces important changes in the temperature field. These changes are manifested through an increase of the fluid and bulk temperatures. It has been found that a higher particle volume concentration clearly induces a decrease of the Nusselt number for the horizontal inclination. On the other hand, for the vertical one, the Nusselt number remains nearly constant with an increase of particle volume concentration from 0 to 4%. Two new correlations have been proposed for computing the asymptotic Nusselt number for a horizontal and a vertical tube. The apparent contradictory behaviour observed between experimental data and analytical/numerical results (fig.10&fig.11) regarding the heat transfer enhancement of nanofluids under buoyant forces has raised serious concerns regarding the applicability of using the single phase and homogeneous fluid model for nanofluids under natural convection effect.

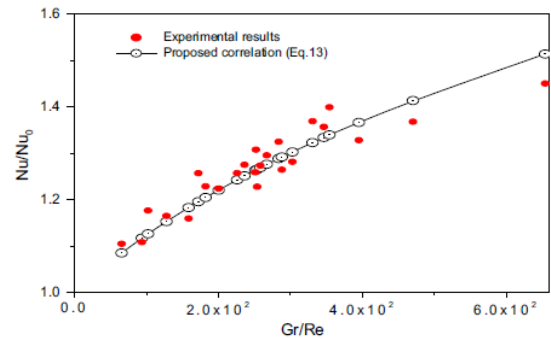


**Fig.10** Relation between Experimental Data & Analytical Data For Vertical Tube.

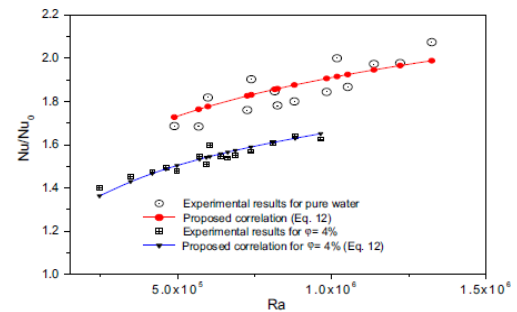


**Fig.11** Comparison between Values Of  $Nu_{\infty}$  Obtained From Experimental Data & Co-Relation For Horizontal Tube.

$$1. \quad Nu = Nu_0(1 - \phi^{0.625})(1 + 5.25 \times 10^{-5} Ra^{1.06})^{0.135} \quad \text{Eq.12}$$

$$2. \quad Nu = Nu_0 \cdot \left(1 + 52.10^4 \frac{Gr}{Re}\right)^{0.28} \quad \text{Eq.13}$$

### 7.2 For second experiment:

The major experimental findings are listed below.

- (i) Heat transfer performance in a straight circular tube is amplified by suspension of Al<sub>2</sub>O<sub>3</sub>-Cu hybrid nanoparticles in comparison with that of pure water. The average increase in Nusselt number for Al<sub>2</sub>O<sub>3</sub>-Cu/water hybrid nanofluid is 10.94% when compared to pure water.
- (ii) The convective heat transfer coefficient increases with increasing Reynolds number. The experimental results of hybrid nanofluid for laminar flow showed a maximum enhancement of 13.56% in Nusselt number at a Reynolds number of 1730 when compared to pure water.
- (iii) The experimental results showed that dilute Al<sub>2</sub>O<sub>3</sub>-Cu/water hybrid nanofluid with 0.1% volume fraction show slightly higher friction factor when compared to pure water. The average increase in friction factor of 0.1% Al<sub>2</sub>O<sub>3</sub>-Cu/water hybrid nanofluids is 16.97% when compared to water. This reveals that dilute Al<sub>2</sub>O<sub>3</sub>-Cu/water hybrid nanofluids will cause extra penalty in pumping power when compared to Al<sub>2</sub>O<sub>3</sub>/water nanofluid.

## References

- [1]. Experimental study of mixed convection with water/Al<sub>2</sub>O<sub>3</sub> nanofluid in inclined tube with uniform wall heat flux R. Ben Mansour a,b,\* , N. Galanis b, C.T. Nguyen c 2010 Published by Elsevier Masson SAS.
- [2]. Effect of Al<sub>2</sub>O<sub>3</sub>-Cu/water hybrid nanofluid in heat transfer S. Suresh a,†, K.P. Venkataraj a, P. Selvakumar a, M. Chandrasekar b 2011 Elsevier Inc.
- [3]. S. Lee, S.U.-S. Choi, Application of Metallic Nanoparticle Suspensions in Advanced Cooling Systems PVP-Vol. 342/MD-Vol. 72. ASME Pub., 1996, pp. 227e234.
- [4]. P. Keblinski, J.A. Eastman, D.G. Cahill, Nanofluids for thermal transport. Mater.Today (2005) 36e44.
- [5]. R. Chein, G. Huang, Analysis of microchannel heat skin performance using nanofluids. Appl. Therm. Eng. 25 (Issues 17e18) (2005) 3104e3114.
- [6]. P. Keblinski, S.R. Phillpot, S.U.S. Choi, J.A. Eastman, Mechanisms of heat flow in suspensions of nano-sized particles (nanofluids). Int. J. Heat Mass Transfer 45(2002) 855e863.
- [7]. J.A. Eastman, S.U.-S. Choi, S. Li, W. Yu, L.J. Thompson, Anomalously increased effective thermal conductivities of ethylene glycol-based nanofluids containing copper nanoparticles. Appl. Phys. Lett. 78 (No 6) (2001) 718e720.
- [8]. Y. Xuan, Q. Li, Heat transfer enhancement of nanofluids. Int. J. Heat Fluid Flow 21 (2000) 58e64.
- [9]. Y. Xuan, W. Roetzel, Conceptions for heat transfer correlation of nanofluids. Int. J. Heat Mass Transfer 43 (2000) 3701e3707.
- [10]. A.R.A. Khaled, K. Vafai, Heat transfer enhancement through control of thermal dispersion effects. Int. J. Heat Mass Transfer 48 (No. 11) (2005) 2172.
- [11]. B.C. Pak, Y.I. Cho, Hydrodynamic and heat transfer study of dispersed fluids with submicron metallic oxide particles. Exp. Heat Transfer 11 (No. 2) (1998) 151e170.
- [12]. X. Wang, X. Xu, S.U.-S. Choi, Thermal conductivity of nanoparticles-fluid mixture. J. Thermophys. Heat Transfer 13 (No. 4) (1999) 474e480.
- [13]. J.A. Eastman, S.U.-S. Choi, S. Li, G. Soyez, L.J. Thompson, R.J. DiMelfi, Novel thermal properties of nanostructured materials. J. Metastable Nanocryst Mater 2-6 (1999) 629e634.
- [14]. C.T. Nguyen, F. Desgranges, G. Roy, N. Galanis, T. Maré, Boucher, S. H. Angue Mintsa, Mesure De Viscosité Pour Nanofluides Al<sub>2</sub>O<sub>3</sub>/Eau e Phénomène D'hystérésis, VIIIème Colloque Franco-Québécois sur la Thermique des Systèmes, (Mai 2007) Montréal, ART-01e01.
- [15]. Q.X. Wang, A.S. Mujumdar, Heat transfer characteristics of nanofluids: a review. Int. J. Therm. Sci. 46 (No.1) (2006) 1e19.
- [16]. Q. Li, Y. Xuan, Convective heat transfer performances of fluids with nanoparticles. Proc. 12th Int. Heat Transfer Conference, Grenoble, France, 2002 483e488.
- [17]. D. Wen, Y. Ding, Experimental investigation into convective heat transfer of nanofluids at the entrance region under laminar flow conditions. Int. J. Heat Mass Transfer 47 (2004) 5181e5188.
- [18]. Y. Yang, Z.G. Zhang, E.A. Grulke, W.B. Anderson, G. Wu, Heat transfer properties of nanoparticle-in-fluid dispersions (nanofluids) in laminar flow. Int. J. Heat Mass Transfer 48 (No. 6) (2005) 1107e1116.
- [19]. K. Khanafer, K. Vafai, M. Lightstone, Buoyancy-driven heat transfer enhancement in a two-dimensional enclosure utilizing nanofluid. Int. J. Heat Mass Transfer 46 (2003) 3639e3653.
- [20]. R. Ben Mansour, N. Galanis, C.T. Nguyen, Developing laminar mixed convection of nanofluids in an inclined tube with uniform wall heat flux. Int. J. Num.Meth. Heat Fluid Flow 19 (n. 2) (2009) 146e164.
- [21]. N. Putra, W. Roetzel, S.K. Das, Natural convection of nano-fluid. Heat Mass Transfer 39 (2003) 775e784.
- [22]. D. Wen, Y. Ding, Natural convective heat transfer of suspension of titanium dioxide nanoparticles (nanofluids). IEEE Trans. Nanotechnol. 5 (3) (2006) 220e227.
- [23]. S.Z. Heris, S.G. Etemad, M.N. Esfahany, Experimental investigation of oxide nanofluids laminar flow convective heat transfer. Int. Commun. Heat Mass Transfer 33 (2006) 529e535.
- [24]. W. Daungthongsuk, S. Wongwises, A critical review of convective heat transfer of nanofluids. Renew. Sustain. Energ. Rev. 11 (2007) 797e817.
- [25]. S. Kakac, R.K. Shah, W. Aung, Handbook of Single Phase Convective Heat Transfer. Wiley, New York, 1987.
- [26]. R. Ben Mansour, N. Galanis, C.T. Nguyen, Developing laminar mixed convection of nanofluids in a horizontal tube with uniform wall heat flux, Proc. 13<sup>th</sup> IHTC, Sydney NSW, Australia, 2006 13e18.

- [27]. B.S. Petukhov, A.F. Polyakov, Effect of free convection on heat transfer during forced flow in a horizontal pipe. High Temp. Res. Ins. 5 (1966) 348e351.
- [28]. R. Ben Mansour, N. Galanis, C.T. Nguyen, Effect of uncertainties in physical properties on forced convection heat transfer with nanofluids. Appl. Therm. Eng. 27 (no. 1) (2007) 240e249.
- [29]. G. Polidori, S. Fohanno, C.T. Nguyen, A note on heat transfer modeling of Newtonian nanofluids in laminar free convection. Int. J. Therm. Sci. 46 (no. 8) (2007) 739e744.
- [30]. R. Ben Mansour, N. Galanis, C.T. Nguyen, Experimental Study of Mixed Convection Laminar Flow of Water-Al<sub>2</sub>O<sub>3</sub> Nanofluid in Horizontal Tube with Uniform Wall Heat Flux. Proc. 5th IASME/WSEAS Int. Conf. on Fluid Mechanics and Aerodynamics, Greece, August 24-26, 2007.